

Time-Resolved Study of Intense Terahertz Pulses Generated by a Large-Aperture Photoconductive Antenna

Toshiaki HATTORI*, Keiji TUKAMOTO and Hiroki NAKATSUKA

Institute of Applied Physics, University of Tsukuba, Tsukuba 305-8573, Japan

(Received March 23, 2001; accepted for publication May 23, 2001)

Saturation behavior of intense terahertz radiation pulses emitted by a large-aperture photoconductive antenna was studied by observing the waveforms of the generated terahertz pulse using the electrooptic sampling method. A peak terahertz field up to 5.7 kV/cm was observed. By increasing the pump pulse fluence, saturation of the peak terahertz field, shift of the peak appearance time and narrowing of the terahertz pulse were observed. These experimental results were found to be qualitatively consistent with the results of simulation based on the current surge model.

KEYWORDS: terahertz, femtosecond, current surge, photoconductive antenna, electrooptic sampling

1. Introduction

Intense electromagnetic pulses in the terahertz (THz) spectral region have been generated by illuminating femtosecond optical pulses on large-aperture biased photoconductors.^{1,2)} You *et al.* reported the generation of high-power THz pulses with pulse energy of as much as 0.8 μJ at a repetition rate of 10 Hz from a GaAs wafer with 3-cm gap electrodes.¹⁾ Budiarto *et al.* have generated 0.4- μJ THz pulses at a 1-kHz repetition rate from a similar large-aperture biased antenna.²⁾ Intense THz pulses have been applied in experiments on ionization of Rydberg atoms,³⁾ and in THz-field-induced second-harmonic generation from molecular liquids.⁴⁾ Many other potential applications of intense THz pulses have been proposed, which include the study of semiconductor carrier dynamics,²⁾ and liquid dynamics.⁵⁾

The mechanism of generation of THz radiation from biased photoconductors is generally understood based on the current surge model.⁶⁾ In this model, a THz electromagnetic field is radiated from a transient current generated on the surface of a photoconductor. Ultrashort optical pulses generate carriers almost instantaneously and the carriers are accelerated by the local electric field. The resultant transient current, or current surge, produces an electric field on the surface of the photoconductor and this surface field can be regarded as the source of the THz radiation. The surface field, at the same time, partly cancels the bias field applied to the photoconductor, which is called the near-field screening effect. Saturation of pulse energy of the generated THz radiation as a function of pump pulse fluence has been observed by several groups of researchers.^{6–9)} A theoretical treatment of the THz radiation generation process incorporating the near-field screening effect has explained these phenomena successfully. These experimental studies, however, used relatively small gap spacings, which ranged from 0.5 mm to 5 mm. The mechanism of saturation of THz radiation from emitters with centimeter-size gaps,^{1,2)} which are required for intense THz field generation, has not been carefully studied yet. The spatial distribution of the bias field between the electrodes is dependent on the size and shape of both the photoconductor and the electrodes. Thus, it is necessary to study terahertz pulse generation from emitters having such large aperture sizes.

Waveform measurement of THz radiation using the elec-

trooptic (EO) sampling method¹⁰⁾ is a powerful tool for the study of intense THz radiation generation. Temporal resolution of this method is only limited by the duration of the optical pulses when an appropriately thin EO crystal is used. Observation of waveforms of THz pulses generated under a saturated condition is the most direct way to study the mechanism of THz radiation generation. The absolute value of the electric field can also be obtained by this method. Pulse energy measurement techniques of THz radiation applying a bolometer or a pyroelectric detector have been used for the study of THz pulse generation using large-aperture antennas.^{1,2)} What is required, however, in many useful applications of intense THz radiation, is not the large pulse energy but a high peak electric field. Since estimation of electric field strength from the pulse energy^{1,2)} is indirect and unreliable, direct measurement of the field using the EO method is desirable.

In this study, we generated intense THz radiation from a large-aperture GaAs photoconductive antenna and observed the waveforms of the field of focused THz radiation using the EO sampling method. Saturation of the peak electric field was observed as the pump pulse fluence was increased and a peak field as high as 5.7 kV/cm was observed. It is observed that the waveform changes with saturation. Experimental results were compared with the simulation results based on the current surge model.

2. Experiments and Results

Time-resolved THz field measurements by the EO method¹⁰⁾ were performed using the experimental setup shown in Fig. 1. The emitter of THz radiation was a non-doped semi-insulating GaAs wafer with a (100) surface. The diameter and thickness of the wafer were 50 mm and 350 μm , respectively. Two aluminum electrodes were mechanically contacted to the wafer with an intergap spacing of 30 mm. A pulsed electrical voltage of up to 20 kV was applied to the electrodes. The duration and the repetition rate of the voltage pulse were 1 μs and 1 kHz, respectively.

The light source used in the experiment consisted of regeneratively amplified femtosecond Ti:sapphire laser pulses (Spitfire, Spectra Physics). The pulse width, pulse energy, wavelength and the repetition rate of the output of the amplifier were approximately 150 fs, 800 μJ , 800 nm and 1 kHz, respectively. A major portion of the amplifier output was used

*E-mail address: hattori@bk.tsukuba.ac.jp

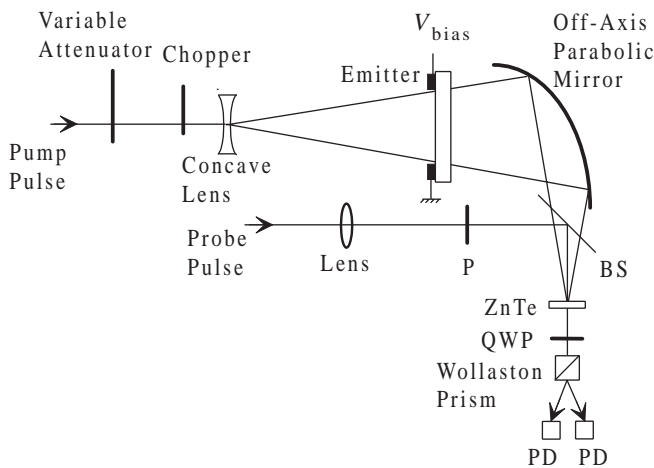


Fig. 1. Schematic of the experimental setup for electrooptic sampling measurement of waveforms of intense THz radiation emitted by a large-aperture photoconductive antenna. BS: pellicle beamsplitter, P: polarizer, PD: photodiode and QWP: quarter-wave plate.

to pump the GaAs emitter. A small portion was split off and used as a probe beam. The pump beam passed through a variable attenuator and was chopped at 500 Hz by a mechanical chopper, which was synchronized to the amplifier output. The beam was expanded by a concave lens with a focal length of 70 mm and incident on an intergap area of 9 cm^2 of the emitter synchronously with the applied high voltage. The distance between the concave lens and the GaAs wafer was about 600 mm.

THz radiation generated from the emitter in the transmission direction was focused by an off-axis parabolic mirror onto a 1.33-mm-thick (110) ZnTe crystal. The focal length and the diameter of the off-axis parabolic mirror were 152 mm and 50 mm, respectively. The distance between the GaAs wafer and the parabolic mirror was about 80 mm. The ZnTe crystal was oriented so that the (001) direction was parallel to the polarization of the THz radiation. In this case, birefringence is induced due to the EO effect of the ZnTe crystal between the light polarization parallel to the THz polarization and that perpendicular to it. In order to detect the birefringence, the probe pulse was set to be linearly polarized in the 45° direction.

The phase difference, $\Delta\theta$, between the light beams having these two polarization directions is expressed as

$$\Delta\theta = \frac{\pi d r_{41} n_0^3}{\lambda} E_{\text{THz}}(t). \quad (1)$$

Here, λ is the wavelength of the probe light and d , r_{41} and n_0 are the thickness, the EO constant and the refractive index of the ZnTe crystal. The values given in literature of $r_{41} = 4.0\text{ pm/V}$ and $n_0 = 2.85$ were used for these parameters for calculating the THz field from the experimental data.^{11,12} If we orient the THz field along the (110) direction, we can double the EO efficiency. In the present study, however, we adopted this orientation in order to reduce the nonlinear contribution since the largest phase difference observed was as much as 0.1.

Probe pulses were reflected by a pellicle beamsplitter and loosely focused on the ZnTe crystal by a lens in a collinear geometry with the THz radiation. Probe pulses which passed

through the ZnTe crystal were transmitted through a quarter-wave plate, and the polarization change due to the EO effect was detected by a combination of a Wollaston prism and a pair of Si photodiodes. The difference of the output of the two photodiodes was sent to a lock-in amplifier and a 500-Hz component was recorded.

A typical waveform of THz radiation obtained by this measurement setup is shown in Fig. 2. This was obtained using a relatively low pump fluence of $2\text{ }\mu\text{J}/\text{cm}^2$ and a bias field of 1 kV/cm. The initial high peak with a width of 690 fs is followed by a negative trailing part which persists for about 8 ps after the appearance of the peak. A small peak which appears around 8 ps is due to the reflection of the main pulse inside the GaAs wafer. Small oscillations in the waveform were reproducible and are attributed to water vapor absorption.¹³ The part before the reflection peak of the waveform shown in Fig. 2 was Fourier transformed. The Fourier amplitude obtained is shown in Fig. 3. The spectrum extended from the dc component to above 2.5 THz. A dip around 1.7 THz is due to water vapor absorption.¹³

The peak field of THz pulses is plotted as a function of the bias field at several values of pump fluence, F , in Fig. 4. It is seen that the peak field is proportional to the bias field within the range of bias field and pump fluence used in the

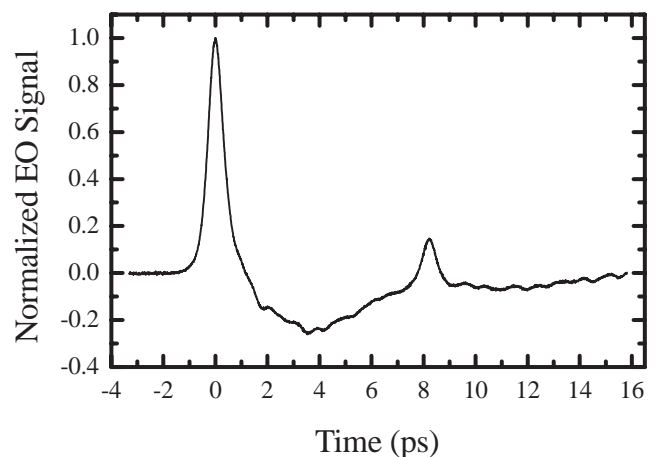


Fig. 2. Typical waveform of focused THz radiation measured by the EO sampling method, obtained at a relatively low pump fluence of $2\text{ }\mu\text{J}/\text{cm}^2$ and bias field of 1 kV/cm.

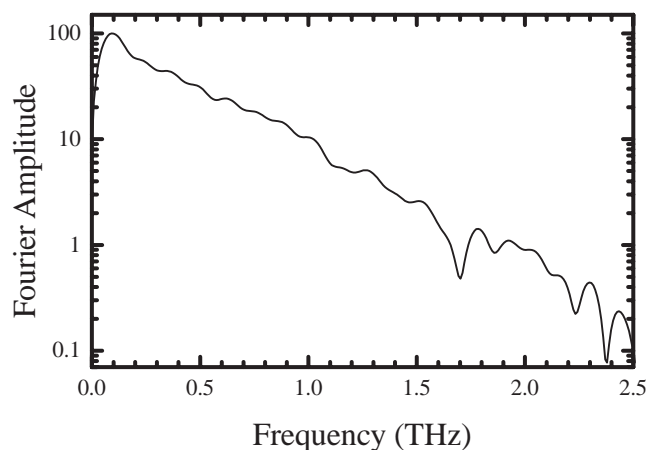


Fig. 3. Fourier amplitude of the waveform shown in Fig. 2.

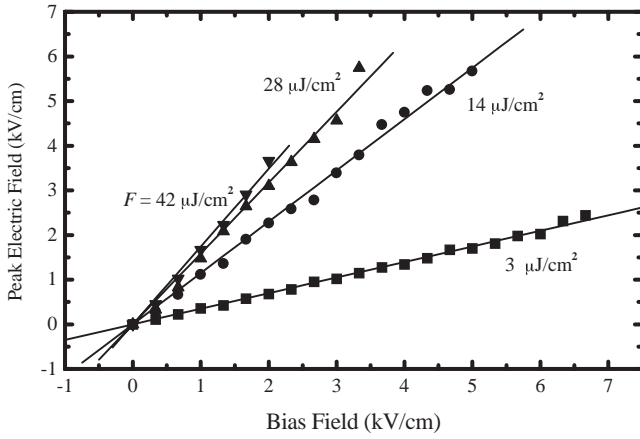


Fig. 4. Bias field dependence of peak THz field at several values of pump fluence.

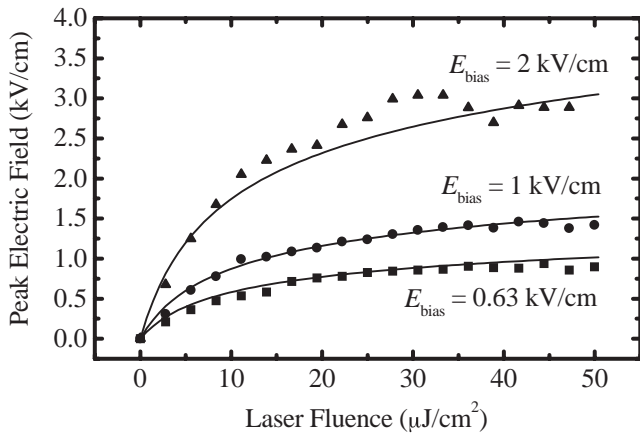


Fig. 5. Pump fluence dependence of peak field of the THz radiation at several values of bias field. Solid lines indicate best fitted curves with the theoretical expression described in §3 with saturation fluence of 7 μJ/cm².

experiment. Waveforms at different bias fields at fixed pump fluence were almost indistinguishable when they were normalized to the peak value. The highest peak field observed in the present experiment was 5.7 kV/cm. The practical limit of the highest peak field achievable was determined by the discharge between the electrodes and the GaAs wafer. The onset of the discharge was dependent on the pump fluence. For smaller fluence, discharge occurred at higher bias field.

Pump fluence dependence of peak THz field is shown in Fig. 5. The peak THz field showed clear saturation behavior as a function of pump fluence. Waveforms of THz radiation around the peak are shown in Fig. 6. Two features are seen in the figure. First, the peak appears earlier when the pump fluence is increased. Second, the pulse becomes narrower with an increase of pump fluence. Pulse widths and peak shifts of these waveforms are plotted in Fig. 7 as a function of pump fluence. The shift of peak appearance time shows almost linear dependence on the pump fluence. On the other hand, pulse width shows a saturation behavior.

3. Theory

In this section, we derive an expression of time-dependent THz field strength at a focused point using the current surge model. The current surge model is widely accepted as a model

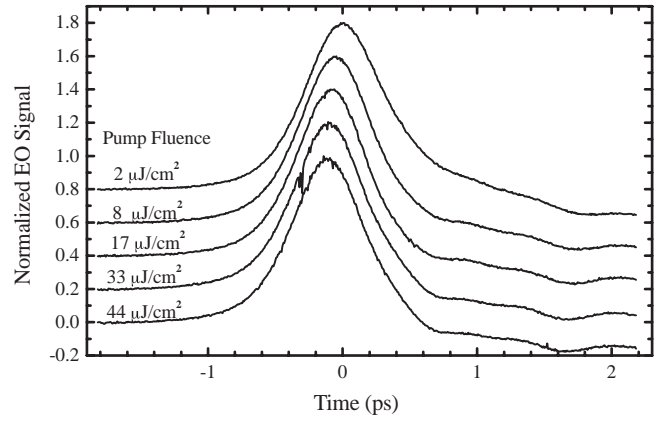


Fig. 6. Waveforms of THz radiation around the peak at several pump fluence values. Each trace is normalized and shifted upward by 0.2.

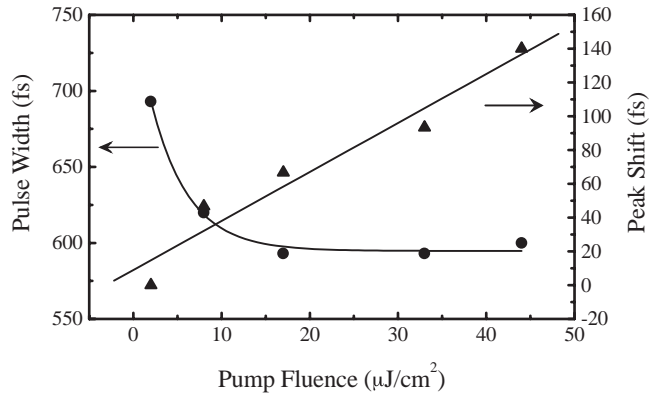


Fig. 7. Experimentally observed pulse width (full-width at half maximum) and shift of peak appearance time are plotted as a function of pump fluence. Solid curves are given only as eye guides.

describing the process of THz radiation generation in biased photoconductors.⁶⁾ In this model, the surface current density $J_S(t)$ of the photoconductive emitter is related to the local applied field by Ohm's law:

$$J_S(t) = \sigma_S(t) [E_{\text{bias}} + E_{\text{surf}}(t)]. \quad (2)$$

Here, $\sigma_S(t)$ is the time-dependent surface conductivity, E_{bias} is the static bias field applied to the emitter and $E_{\text{surf}}(t)$ is the waveform of the generated THz radiation field observed on the surface of the emitter. From the boundary conditions of Maxwell's equations, $E_{\text{surf}}(t)$ is related to $J_S(t)$ as

$$E_{\text{surf}}(t) = -\frac{\eta_0}{1 + \sqrt{\epsilon}} J_S(t), \quad (3)$$

where $\eta_0 = 377 \Omega$ is the impedance of vacuum and ϵ is the dielectric constant of the emitter medium. From eqs. (2) and (3), an expression for $E_{\text{surf}}(t)$ is obtained as

$$E_{\text{surf}}(t) = -\frac{\sigma_S(t)\eta_0}{\sigma_S(t)\eta_0 + (1 + \sqrt{\epsilon})} E_{\text{bias}}. \quad (4)$$

The value of E_{surf} shows saturation for a large value of σ_S due to the cancellation of the local bias field by the surface field as seen in eq. (2).

Surface conductivity, $\sigma_S(t)$, is given by the following expression:

$$\sigma_S(t) = e\mu N(t). \quad (5)$$

Here, e is the elementary charge and μ is the electron mobility. Mobility of holes is neglected here since it is generally much smaller than that of electrons. Carrier density, $N(t)$, is given by

$$N(t) = \frac{1-R}{h\nu} \int_{-\infty}^t I(t') dt'. \quad (6)$$

Here, R is the reflectance of the emitter for the pump light, ν is the frequency of the pump light and $I(t)$ is the pump intensity. It is assumed here that decay of the carrier density due to recombination or trapping is slow and can be neglected in the time window of interest. The value of the surface field after illumination of the pump pulse is expressed as

$$E_{\text{surf}}(\infty) = -\frac{F}{F+F_{\text{sat}}} E_{\text{bias}}, \quad (7)$$

where

$$F = \int_{-\infty}^{\infty} I(t) dt \quad (8)$$

is the pump fluence and the saturation fluence, F_{sat} , is defined by

$$F_{\text{sat}} = \frac{h\nu(1+\sqrt{\epsilon})}{e\mu\eta_0(1-R)}. \quad (9)$$

The electric field of the focused terahertz pulse, $E_{\text{focus}}(t)$, has been shown to be proportional to the time derivative of the surface field.⁹⁾ By assuming the pulse shape of the pump light to be Gaussian as

$$I(t) = \frac{F}{\sqrt{\pi}\delta t} \exp(-t^2/\delta t^2), \quad (10)$$

it can be shown that the focused field is proportional to the normalized focused field, $\tilde{E}_{\text{focus}}(t)$:

$$\tilde{E}_{\text{focus}}(t) = \frac{(F/F_{\text{sat}}) \exp(-t^2/\delta t^2)}{[(F/F_{\text{sat}})\Phi(t/\delta t) + 1]^2}. \quad (11)$$

Here, the function $\Phi(x)$ is defined by

$$\Phi(x) \equiv \frac{1}{\sqrt{\pi}} \int_{-\infty}^x \exp(-s^2) ds. \quad (12)$$

Finally, an expression for the normalized surface field is obtained as

$$E_{\text{surf}}(t)/E_{\text{bias}} = -\frac{(F/F_{\text{sat}}) \Phi(t/\delta t)}{(F/F_{\text{sat}}) \Phi(t/\delta t) + 1}. \quad (13)$$

Waveforms of the surface field and the focused THz field simulated using eqs. (13) and (11) are plotted in Figs. 8 and 9, respectively, with several values of normalized pump fluence, F/F_{sat} . It is clearly seen from Fig. 9 that the value of the peak THz field saturates as a function of the pump fluence, the peak position is shifted temporally to the negative direction, and the pulse width is narrowed by increasing the pump fluence. These features can be explained by examining Fig. 8 since the focused THz field waveform is proportional to the time derivative of the surface field waveform. Saturation of the focused field is primarily due to the saturation of the surface field. Under a saturated condition, the surface field rises earlier and more rapidly than under an unsaturated condition, which explains the peak shift and pulse narrowing observed with the focused field waveforms. The peak values of the

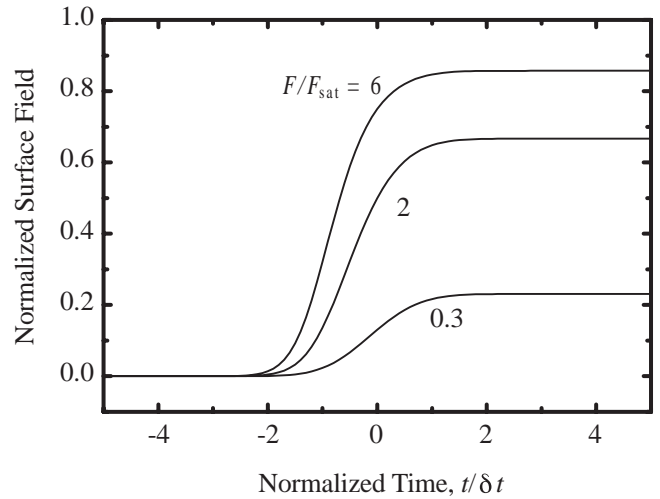


Fig. 8. Simulated time dependence of normalized surface field with several values of normalized pump fluence, F/F_{sat} .

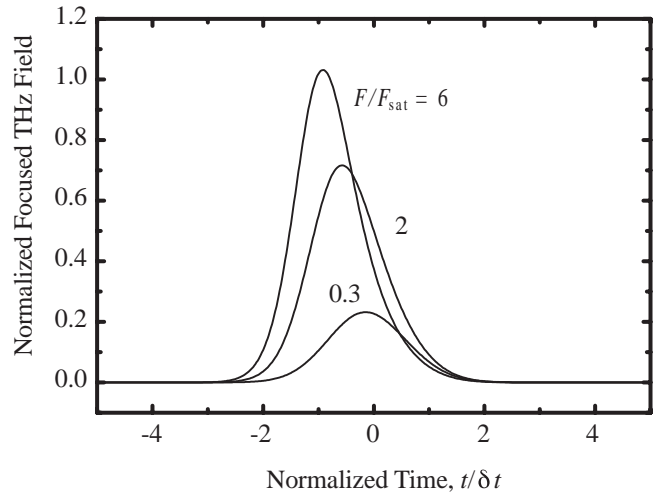


Fig. 9. Simulated waveforms of normalized focused THz radiation at several values of normalized pump fluence.

normalized focused field, pulse width (full-width at half maximum), and peak position calculated from eq. (11) are plotted in Figs. 10 and 11 as a function of the normalized fluence. In Fig. 10, the maximum value of the normalized surface field, $E_{\text{surf}}(\infty)/E_{\text{bias}}$, is also shown by a dotted line along with the normalized peak field of focused THz radiation.

4. Discussion

According to the current surge model discussed in the preceding section, the waveform of focused THz radiation under unsaturated condition should be proportional to the temporal profile of the intensity of the pump pulse. However, the observed EO signal, as shown in Fig. 2, shows marked differences from the temporal profile of the 150-fs pump pulse. First, the main peak is much wider than the pump pulse width. Second, there is a negative trailing part. These features have also been observed by other groups of researchers in experiments using setups similar to the present one.^{4,14,15)} In the far-field regime, it is natural to conceive that the waveform has a bipolar feature because the integrated average field must go

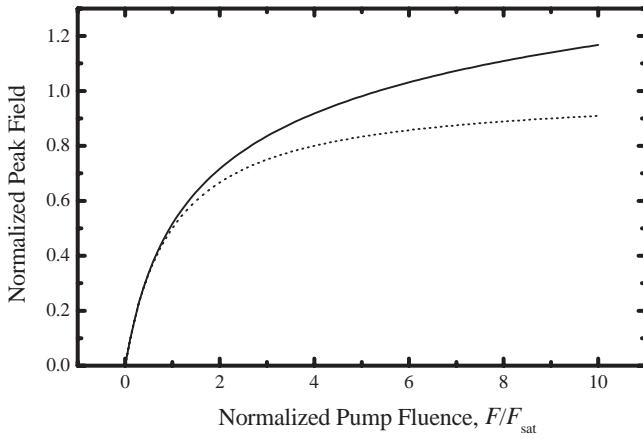


Fig. 10. Normalized peak value of the focused THz field (solid line) and that of the surface field (dotted line) as a function of the pump fluence, the values of which are obtained by the calculation.

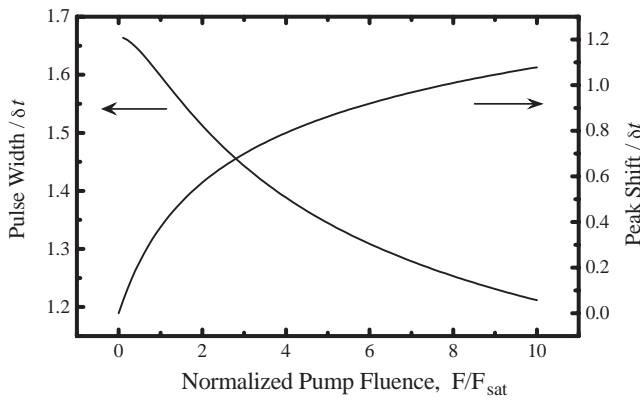


Fig. 11. Pulse width and shift of the peak position of the focused THz field as a function of the pump fluence, the values of which are obtained by the calculation.

to zero (no dc component). This simple idea cannot explain the observed waveform since the time integration of the waveform yields a large negative value. Furthermore, the experimental condition does not satisfy the far-field criteria. The observation time window of about 20 ps corresponds to a frequency of 50 GHz or a wavelength of 6 mm. The confocal parameter of a beam with this wavelength and a beam waist of 3 cm is about 11 cm, which is of the same order as the distance between the emitter and the observation point. This shows that the waveform was detected still in the near field regime. In the theoretical treatment mentioned in the preceding section, the focused THz field was assumed to be proportional to the time derivative of the surface field, which is only valid for sufficiently high frequency components.¹⁶⁾ The contribution of low-frequency components to the THz waveform was neglected in this treatment. Under the actual experimental conditions, the contribution of low-frequency components to the waveforms of the THz radiation cannot be neglected and the amplitude and phase of low-frequency components can be affected by imperfect experimental conditions such as the finite size of the GaAs wafer, the large distance between the GaAs wafer and the parabolic mirror and the finite size of the parabolic mirror. Therefore, the negative long tail observed in the experimentally obtained waveforms should be attributed to the low-frequency contribution which cannot be

treated in an exact manner by the simple theoretical treatment of the present study.

The broadening of the main peak, on the other hand, is attributed to the dynamical processes of electrons in the GaAs wafer. Although the time resolution of the EO sampling method is limited by several factors such as finite duration of the probe pulse, dispersion of the THz radiation and the optical probe pulse and the velocity mismatch between them, the experimentally observed broadening of the peak from 150 fs to 600–700 fs cannot be explained by these factors. Spectra of the THz radiation generated by similar setups have been observed.^{1,2)} These spectra also suggest pulse widths of about 500 fs. By the 800-nm pump pulse, electrons in GaAs are excited to the conduction band with an extra energy of 120 meV. The time required for the electrons with this extra energy to relax down to the conduction band minimum has been estimated to be 500–600 fs.¹⁷⁾ This is supported by the experimental observation on the time dependence of the electron mobility of GaAs immediately after excitation by femtosecond optical pulses.¹⁸⁾ Revisions of the simple current surge model used in this study by incorporating the time dependence of the electron mobility have been presented.^{17,19,20)} These theoretical treatments have succeeded partly in explaining the broadening of THz pulses, as observed in the present experiment.

Furthermore, the typical value of electron mobility of GaAs at $\mu = 5000 \text{ cm}^2/\text{V}\cdot\text{s}$ indicates an electron scattering time of $\tau_{sc} = 190 \text{ fs}$, which is obtained from the relationship:

$$\tau_{sc} = \frac{\mu m_e^*}{e}. \quad (14)$$

Here, the effective mass of electrons was assumed to be $m_e^* = 0.067 m_e$. Since electron scattering time is the time required to accelerate electrons to the steady-state velocity, this can be another factor which broadens the pulse width of generated THz radiation.

In this paper, we will not discuss the details of carrier dynamics in the emitter medium. Instead, we will introduce an effective pump pulse width, τ_{eff} , which represents the time required for the electrons to be accelerated to the steady-state velocity, in the place of the pump pulse width, t_p . The value of τ_{eff} around 500 fs explains the THz pulse width observed in the present and other studies.

The linear dependence of the THz peak field on the bias field, as seen in Fig. 4 and the fact that no changes were observed in the THz waveforms at different bias fields are consistent with the current surge model described in the preceding section. Nonlinearity in the electron mobility at a local field higher than 4 kV/cm has been predicted by Monte Carlo simulations.²¹⁾ However, results of experimental studies on transient velocity overshoot of electrons in GaAs suggest that this effect is reduced for electrons which are photoexcited above the conduction band minimum.^{22,23)}

The saturation behavior of the THz peak field as a function of pump fluence, as shown in Fig. 5, is essentially similar to that observed using emitters with relatively small aperture sizes.^{6–9)} All the experimental data were well simulated by the theoretical dependence of the peak field on the pump fluence, as plotted in Fig. 10, using the same parameters. The simulated curves are shown in Fig. 5 by solid lines. The saturation fluence obtained by the simulation is $F_{sat} = 7 \mu\text{J}/\text{cm}^2$. Using

this value, electron mobility was calculated from eq. (9) to be $\mu = 4000 \text{ cm}^2/\text{V}\cdot\text{s}$. The value of $\epsilon = 13$ was used for the calculation. This mobility value seems reasonable for electrons photoexcited to slightly above the conduction band minimum of GaAs.

The peak shift and narrowing of the THz pulses observed in the experiment, as shown in Fig. 7, are qualitatively consistent with the theoretical results shown in Fig. 11. Although the quantitative agreement between them is not very good, this observation shows that the present simple theoretical treatment based on the current surge model can be used to explain and predict waveforms of focused intense THz radiation under saturated conditions by replacing the pump pulse width by the effective pulse width, τ_{eff} .

5. Conclusions

We have observed waveforms of focused intense THz radiation emitted by a large-aperture GaAs antenna using the EO sampling method. A peak THz field up to 5.7 kV/cm was observed. By increasing the pump pulse fluence, saturation of the peak THz field, shift of the peak appearance time and narrowing of the THz pulse were observed. The peak field was found to show a linear dependence on the bias field applied to the antenna. Theoretical treatment based on the current surge model has been developed. The experimental observations were explained under this theoretical framework by introducing the effective pump pulse width.

Acknowledgements

This study was partly supported by the Research Foundation for Opto-Science and Technology, and by the Grant-in-Aid for Scientific Research from the Japan Society for the Promotion of Science.

- 1) D. You, R. R. Jones, P. H. Bucksbaum and D. R. Dykaar: *Opt. Lett.* **18** (1993) 290.
- 2) E. Budiarto, J. Margolies, S. Jeong, J. Son and J. Bokor: *IEEE J. Quantum Electron.* **32** (1996) 1839.
- 3) R. R. Jones, D. You and P. H. Bucksbaum: *Phys. Rev. Lett.* **70** (1993) 1236.
- 4) D. J. Cook, J. X. Chen, E. A. Morlino and R. M. Hochstrasser: *Chem. Phys. Lett.* **309** (1999) 221.
- 5) K. Okumura and Y. Tanimura: *Chem. Phys. Lett.* **295** (1998) 298.
- 6) J. T. Darrow, X.-C. Zhang, D. H. Auston and J. D. Morse: *IEEE J. Quantum Electron.* **28** (1992) 1607.
- 7) J. T. Darrow, X.-C. Zhang and D. H. Auston: *Appl. Phys. Lett.* **58** (1991) 25.
- 8) P. K. Benicewicz and A. J. Taylor: *Opt. Lett.* **18** (1993) 1332.
- 9) P. K. Benicewicz, J. P. Roberts and A. J. Taylor: *J. Opt. Soc. Am. B* **11** (1994) 2533.
- 10) A. Nahata, A. S. Weling and T. F. Heinz: *Appl. Phys. Lett.* **69** (1996) 2321.
- 11) T. R. Sliker and J. M. Jost: *J. Opt. Soc. Am.* **56** (1966) 130.
- 12) D. T. F. Marple: *J. Appl. Phys.* **35** (1964) 539.
- 13) J. Kauppinen, T. Kärkkäinen and E. Kyrö: *J. Mol. Spectrosc.* **71** (1978) 15.
- 14) C. Winnewisser, F. Lewen and H. Helm: *Appl. Phys. A* **66** (1998) 593.
- 15) C. Winnewisser, F. Lewen, J. Weinzierl and H. Helm: *Appl. Opt.* **38** (1999) 3961.
- 16) T. Hattori, R. Rungsaawang, K. Tukamoto and H. Nakatsuka: in preparation.
- 17) A. Gürtler, C. Winnewisser, H. Helm and P. U. Jepsen: *J. Opt. Soc. Am. A* **17** (2000) 74.
- 18) M. C. Nuss, D. H. Auston and F. Capasso: *Phys. Rev. Lett.* **58** (1987) 2355.
- 19) A. J. Taylor, P. K. Benicewicz and S. M. Young: *Opt. Lett.* **18** (1993) 1340.
- 20) G. Rodriguez, S. R. Caceres and A. J. Taylor: *Opt. Lett.* **19** (1994) 1994.
- 21) J. G. Ruch: *IEEE Trans. Electron Devices* **19** (1972) 652.
- 22) J. Son, W. Sha, J. Kim, T. B. Norris, J. F. Whitaker and G. A. Mourou: *Appl. Phys. Lett.* **63** (1993) 923.
- 23) J.-H. Son, T. B. Norris and J. F. Whitaker: *J. Opt. Soc. Am. B* **11** (1994) 2519.